A molecular switch in mouse CD1d modulates natural killer T cell activation by α-galactosylsphingamides

Jing Wang[1*], Joren Guillaume[2*], Jonas Janssens[2], Soumya G. Remesh[1], Ge Ying[1], Aruna Bitra[1], Serge Van Calenbergh[2,*], and Dirk M. Zajonc[1,3,^,*]

[1]Division of Immune Regulation, La Jolla Institute for Allergy and Immunology (LJI), La Jolla, CA 92037, USA.

[2]Laboratory for Medicinal Chemistry (FFW), Faculty of Pharmaceutical Sciences, and [3]Department of Internal Medicine, Faculty of Medicine and Health Sciences, Ghent University, 9000 Ghent, Belgium.

[*]Joint first authors, * joint senior authors

Running title: Sphingamide recognition by NKT cells

^To whom correspondence should be addressed: Dirk M. Zajonc, E-mail: Dirk.Zajonc@pfizer.com, Cancer Immunology Discovery, Pfizer, San Diego, CA 92121, USA.

Keywords: glycolipid, antigen presentation, major histocompatibility complex (MHC), T-cell receptor (TCR), cellular immune response, natural killer T cell activation, immune signaling, glycoprotein structure, X-ray crystallography, α-galactosylceramide (α-GalCer)

ABSTRACT

Type I Natural Killer T (NKT) cells are a population of innate like T lymphocytes that rapidly respond to α-GalCer presented by CD1d, via the production of both pro and anti-inflammatory cytokines. While developing novel α-GalCer analogs that were meant to be utilized as potential adjuvants due to their production of pro-inflammatory cytokines (Th1 skewers), we generated α-galactosylsphingamides (α-GSA). Surprisingly, α-GSAs are not potent antigens *in vivo* despite their strong T-cell receptor (TCR)-binding affinities. Here, using surface plasmon resonance (SPR), antigen presentation assays, and X-ray crystallography (yielding crystal structures of 19 different binary [CD1d–glycolipid] or ternary [CD1d–glycolipid–TCR] complexes at resolutions between 1.67 and 2.85 Å), we characterized the biochemical and structural details of α-GSA recognition by murine NKT cells. We identified a molecular switch within murine (m)CD1d that modulates NKT cell activation by α-GSAs. We found that the molecular switch involves a hydrogen bond interaction between Tyr-73 of mCD1d and the amide group oxygen of α-GSAs. We further established that the length of the acyl chain controls the positioning of the amide group with respect to the molecular switch and works synergistically with Tyr-73 to control NKT cell activity. In conclusion, our findings reveal important mechanistic insights into the presentation and recognition of glycolipids with polar moieties in an otherwise apolar milieu. These observations may inform the development α-GSAs as specific NKT cell antagonists to modulate immune responses.

Type I or semi-invariant Natural Killer T (NKT) cells are a specialized population of T lymphocytes that express a semi-conserved TCR α-chain rearrangement (TRAV11/TRAJ18 (Vα14Jα18) in mice, TRAV10/TRAJ18 (Vα24Jα18) in humans) (1). They are restricted by the non-polymorphic and non-classical Major Histocompatibility Class (MHC) I analog CD1d and recognize synthetic, self, and microbial glycolipid antigens (2-14). NKT cells are considered innate like T lymphocytes and respond to antigen challenge within 2-4 hours, producing copious amounts of both pro- and anti-inflammatory cytokines. Many α-GalCer analogs have been studied that induce a superior production of IFN-γ, often combined with a

reduced amount of IL-4 in comparison to α-GalCer itself (aka Th1 skewing)(15-17). It has been observed that Th1 skewing antigens also lead to increased production of IL-12 by the presenting DC, which together with IFN-γ from the NKT cell trans-activate NK cells (18-20). NK cells are the major producers of IFN-γ at later time points. As such NKT cells are of therapeutic interest because they exert a central role in bridging the innate and adaptive immune system. The mechanism of Th1 cytokine skewing involves TCR ligation with CD1d-antigen complexes on DCs, which induces upregulation of costimulatory molecules, such as CD40L on the NKT cell and CD40 on the DC, ultimately leading to DC maturation and IL-12 production. Several non-mutually exclusive mechanisms have been proposed for the Th1 skewing activity of various α-GalCer analogs. These involve the loading of glycolipids to CD1d located in lipid rafts or an increased *in vivo* half-life of CD1d-glycolipid complexes often via enhanced CD1d-glycolipid interactions (16,17,21).

We have previously hypothesized that α-GalCer analogs that contain aromatic groups to enhance binding to CD1d, while not altering TCR recognition are superior Th1 skewing antigens (16). In one of these glycolipids, NU-α-GalCer, the C6"-OH of the galactose was replaced by a naphthyl urea group that induced a structural change in the A' roof of CD1d, leading to a cavity in which the aromatic group is bound (16). In addition to the two lipid tail "anchors", we proposed this novel interaction as the "third anchor" hypothesis (16). Several other α-GalCer analogs that had aromatic groups at the 6"-OH of the galactose also caused an increased serum IFN-γ and IL-12 production, albeit not inducing a structural change within the A' roof, but rather mediating hydrophobic contacts with CD1d or the TCR (17). Other strong Th1 skewing ligands include 7DW8-5, containing a terminal aromatic *para*-fluoro-phenyl group in the acyl chain, and other ligands with terminal phenyl anchors in the acyl chain that bound within the A' pocket of CD1d are currently being tested as vaccine adjuvants (22-26). The sphingosine chain of α-GalCer is the only moiety that had not been systematically substituted with aromatic anchors. We have recently synthesized a panel of α-GalCer analogs in which terminal or in-chain phenyl groups are incorporated in the phytosphingosine moiety of short chain α-GalCer (PBS-25, (27)) via an amide linker (28). These short-chain α-galactosylsphingamides (α-GSA) were bound by the TCR with high affinity, yet did not induce a robust cytokine production when administered to mice by intraperitoneal injection (28). However, when increasing the length of the acyl chain to 26 carbons, α-GSAs induced the production of both the pro- and anti-inflammatory cytokines IL-4 and IFN-γ respectively, albeit at markedly reduced levels compared to α-GalCer (28). In the current study, we have systematically analyzed these α-GSAs with regard to the TCR binding kinetics and their ability to activate a murine iNKT cell hybridoma. We also determined the crystal structures of 19 different binary (CD1d-glycolipid) or ternary (CD1d-glycolipid-TCR) complexes in an effort to unravel the molecular basis of the reduced antigenicity of the α-GSAs. We have discovered that the activity of α-GSAs is regulated by an interplay of acyl chain length and a molecular switch within CD1d that forms a novel interaction with the amide group in the phytosphingosine of α-GSAs.

RESULTS

α-galactosyl sphingamide overview- We have previously reported a novel class of α-GalCer derivatives termed α-galactosylsphingamides (αGSAs) or in short sphingamides (28). The sphingamides are similar to α-GalCer but feature an amide group within the sphingosine moiety at a fixed distance from the anomeric carbon (Figure 1). This amide was used to introduce either a terminal or in-chain phenyl group in the sphingosine. The acyl chain length was varied from eight to twenty-six carbons. We have synthesized various control compounds that mimic the overall structure of the sphingamides but lack the central amide group to assess the influence of this polar moiety in NKT cell activation.

SPR studies using the Vα14Vβ8.2 TCR (clone 2C12)- In analogy to our previous study (28), all sphingamides with a terminal phenyl group were bound by the Vα14Vβ8.2 TCR with similar high affinities in the range from 16 to 37 nM (Figure 2). There were no significant differences between the TCR association and dissociation rates. However, the sphingamide αGSA[26,P5*p*], which has a C26 fatty acid and an in-chain para-substituted phenyl moiety was bound by the TCR with considerably weaker affinity, suggesting that the phenyl moiety impairs TCR binding to CD1d. We have not measured the TCR binding affinities for all sphingamides or control compounds, since our selected lipids establish a similar TCR binding recognition. However, we failed to detect any TCR binding to αGSA[8,2P] and αGSA[8,4P], suggesting that these relatively short sphingamides do not bind to CD1d. This is also corroborated by our inability to obtain crystal structures of these two lipids in complex with CD1d (see below).

iNKT cell activation by sphingamides- Previously we reported that sphingamides are not potent agonists for murine iNKT cells *in vivo* (28). Therefore, we have assessed in detail the antigenicity of sphingamides using a cell free and cell-based antigen presentation assay. Surprisingly, despite their high TCR binding affinity, none of the short acyl chain sphingamides were able to robustly activate the iNKT cell hybridoma 1.2 when presented by recombinant mouse CD1d, suggesting that solely varying the position of the phenyl anchor does not affect antigenicity (Figure 3A). In contrast, short acyl chain α-GalCer (αGC[8,18]) strongly activated iNKT cells. We next investigated whether the sphingamide modification influenced loading in cellular compartments and presentation by CD1d. Therefore, we used a cell-based antigen-presentation assay in which A20 cells were transfected with either wild-type or "tail-deleted" mCD1d (Figure 3B and C). The "tail deleted" mCD1d lacks the tyrosine containing trafficking motif within the cytoplasmic tail and prevents its recycling through lysosomal compartments after mCD1d has been expressed on the cell surface, while wild-type mCD1d can recycle through lysosomal compartments allowing for lipid loading and/or processing. Again, none of the short-chain sphingamides activated iNKT cells, regardless of whether mCD1d had access to lysosomes for potential sphingamide loading using lipid transfer proteins. To increase the binding affinity of the sphingamides to mCD1d, we then synthesized and analyzed the two full-length sphingamides αGSA[26,18P] and αGSA[26,2P5*p*]. Surprisingly, both lipids potently activated iNKT cells and the response was optimal already at the lowest lipid concentration (0.5 µg/ml), despite αGSA[26,2P5*p*] having a 10-fold reduced TCR binding affinity (Figure 2 and 3D). The antigen-presentation data led us to hypothesize that the acyl chain length influences iNKT cell activation by sphingamides and, therefore, we have also generated and included intermediate acyl chain αGSAs (C12, C16, and C20) in our subsequent studies. Theses αGSAs were based on the sphingamide 6P backbone.

Sphingamide presentation by CD1d- In order to rationalize why all sphingamides are bound by the iNKT TCR with high affinity, but only long acyl chain sphingamides potently activate iNKT cells, we examined the structural basis of sphingamide presentation by mCD1d. The individual crystal structures of mCD1d-sphingamide complexes were determined to resolutions between 1.67 Å and 2.45 Å (Table S1). The two short-chain sphingamides αGSA[8,6P] and αGSA[8,8P] had been crystallized previously (termed as 5d and 5e in (28)). Most sphingamides show well-defined electron density for the hydroxyls of both the sugar moiety and the lipid backbone, indicative of an ordered presentation by CD1d (Figure 4).

The exception was αGSA[12,6P], which showed well-defined electron density for the galactose but less ordered electron density around the amide group, suggesting a more flexible binding of that portion. As expected for a-GalCer analogs, the acyl chain is always inserted into the A' pocket, regardless of its length, while the sphingosine moiety containing the amide group is bound in the F' pocket. Up to an acyl chain length of C12, all sphingamides also recruited a spacer lipid into the A' pocket of CD1d. Interestingly the helical orientation of the acyl chain circling in the A' pocket differs between the longer sphingamides αGSA[20,6P] and αGSA[26,6P]. While αGSA[20,6P] circles clockwise when looking down at the pocket, αGSA[26,6P] circles in a counter-clockwise fashion. Whether there is a functional consequence of the acyl chain binding orientation is not known.

The sphingamide αGSA[8,6P] was structure-based designed and predicted to form an additional hydrogen-bond between its amide oxygen and the hydroxyl of mCD1d residue Tyr73. Surprisingly, only the long chain sphingamide αGSA[26,6P] exhibited this H bond, while the amide group of the shorter homologues and other sphingamides exhibit an altered orientation (Figure 5). It appears there is a high degree of rotational freedom for this group, with the amide oxygen either pointing towards or away from Tyr73. However, since the electron density in that region is well-defined for most sphingamides, we propose that the acyl chain length influences the precise positioning of the amide group in the F' pocket, which in turn influences iNKT cell activation. Except for the amide group, the sphingamides bound in a conserved orientation with the galactose being stabilized by a core hydrogen bond network involving CD1d residues Asp80, Asp153, and Thr156 and the 2"-OH, 3"-OH of the galactose as well as the 3'- and/or 4' hydroxyls of the phytosphingosine chain. The only exception is αGSA[20,6P] which showed a slight rotation in the galactose positioning. This binding orientation resulted in the loss of the H bond interaction between Asp153 of CD1d and 2"-OH and 3"-OH of the galactose, while a new H bond is formed with the 4"-OH. However, the electron density for the galactose of this ligand is less contoured compared to other sphingamides, suggesting some flexibility in the binding orientation, especially since there is no well-defined electron density for the galactose hydroxyls (Figure 4).

TCR recognition of sphingamides- Since we had previously established that the TCR of iNKT cells can induce a structural change in both glycolipid as well as mCD1d upon binding (29), we also determined the crystal structures of a panel of sphingamides presented by mCD1d and in complex with the Vα14Vβ8.2 TCR (clone 2C12) at resolutions between 2.0 Å and 2.85 Å (Table S1). The TCR binds above mCD1d in the canonical parallel binding orientation, with the complementarity-determining region (CDR) 1α sitting above the galactose of the glycolipids and CDR3α binding centered above the F' pocket of CD1d. CDR3α both contacted the glycolipid ligand, as well as the F' roof using the hydrophobic finger Leu99α (Figure 6).

The electron density of each glycolipid is unambiguous, even in the lower resolution structures and is a consequence of the TCR stabilizing and locking the binding orientation of the glycolipids inside the CD1d binding groove. A close examination of the CD1d-glycolipid, as well as TCR-glycolipid interactions reveals no differences between the different sphingamides, in contrast to the binary complexes, in which the sphingamides bind differently to mCD1d with respect to the positioning of the amide group in the phytosphingosine-like moiety. The TCR forms the canonical hydrogen bond interactions, especially Gly96α with the 2"-OH and Asn31α with the 3"- and 4"-OH groups of the galactose, while Arg95α contacts Asp80 of CD1d (Figure 7). In the ternary complexes, all sphingamides, regardless of whether they contain a central or terminal phenyl attached to the amide group within the phytosphingosine-like moiety, now form an additional H bond between the hydroxyl of Try73 of CD1d and the amide oxygen of the sphingamides. This suggests that upon TCR binding, the TCR forces each sphingamide into a conserved binding orientation, the hallmark of which is the formation of this novel H bond interaction.

Identification and characterization of a molecular switch in CD1d- Given the fact that the long chain sphingamide agonist αGSA[26,6P] has the identical binding orientation in the ternary complex compared to the inactive short chain sphingamide αGSA[8,6P], we compared the binding orientation before and after TCR binding for all crystallized sphingamides (Figure 8A and B). Surprisingly, only the active sphingamide αGSA[26,6P] shows the additional H bond with Tyr73 of CD1d in the absence of TCR binding (Figure 8A), while all sphingamides form this H bond upon TCR binding (Figure 8B). This led us to speculate that the length of the acyl chain determines the binding orientation of the amide group in the F′ pocket of CD1d, and whether or not it is further stabilized by the additional H bond with Tyr73. We hypothesize that this interaction forms a molecular switch that affects sphingamide activity. A preformed H-bond (in the absence of TCR) resembles an active state ("switch ON"), while lack of this H bond will lead to an inability of activating iNKT cells ("switch OFF"). A systematic analysis of a panel of sphingamides with increasing acyl chain length revealed a direct correlation between acyl chain length and antigenicity. The short C8 acyl chain failed to robustly activate an iNKT cell hybridoma in a cell-free antigen presentation assay using recombinant mCD1d, while the antigenicity successively increases with increasing acyl chain length (Figure 8C). This suggests that the presence or absence of the pre-formed H bond involving Tyr73 are the two extreme states (ON *vs.* OFF) and that the acyl chain length modulates the overall intrinsic activity of sphingamides. We have further tested the influence of the H-bond by site-directed mutagenesis of the molecular switch (Tyr73). Tyr73Phe-modified CD1d retains its overall structure and interaction with sphingamide, while excluding H bond bond formation with the amide. With the exception of the long chain sphingamide αGSA[26,6P], the activity of all sphingamides is markedly reduced, suggesting that the H bond stabilizes the binding orientation of the amide group within CD1d after TCR binding to allow for potent iNKT cell activation. However, the H bond itself is not the only driver of activity. The acyl chain length itself dictates the binding orientation of the amide group even in the absence of this stabilizing H bond. The Tyr73Phe mutant also showed slightly decreased cytokine production by the control antigen αGC[8,18] but not to the extend observed for the sphingamides. We next speculated that modifying the molecular switch to stabilize the orientation of the amide group in the "ON position" would increase antigenicity. Hereto, we generated the mutant mCD1d Tyr73His. Indeed, all sphingamides now show hyperactivity, even the otherwise inactive short chain αGSA[8,6P], while in contrast the activity of the control antigen was greatly reduced (~4-fold) (Figure 8C). This suggests that introducing a polar group into an apolar environment (the hydrophobic F' pocket of CD1d) reduces the activity of traditional hydrophobic glycolipid antigens, while it is beneficial for engineered glycolipids that contain polar groups within the sphingosine chain.

The polarity likely stabilizes the amide group and positions it away from the F' roof, which is the major binding site of the TCRα chain, especially the hydrophobic finger Leu99a, which was shown to be

crucial for iNKT cell activation (30). If our hypothesis holds true, we would expect that the inactive sphingamide αGSA[8,6P] now forms the additional H bond with His73 in the mCD1d Tyr73His mutant before TCR binding, leading to an active complex. We have, therefore, determined the crystal structure of the mCD1d Tyr73His/αGSA[8,6P] complex (Table S1 and Figure 8D). As expected, αGSA[8,6P], which had the amide oxygen pointing away from the hydroxyl of Tyr73 in wildtype CD1d ("switch OFF") (Figure 8A, yellow lipid), now features a rotated amide group to form an H bond with His73 ("switch ON"). Electron density in that region is unambiguous, however, the introduction of polarity in the F' pocket slightly affects binding of the terminal acyl chain carbons in the A' pocket, for which electron density becomes disordered.

In summary, two factors appear to drive sphingamide activity. The acyl chain length, which dictates amide positioning within CD1d and the ability to form a stabilizing interaction with Tyr73 to lock the binding orientation of the amide group in an active state.

DISCUSSION

In this study, we have characterized a panel of α-GalCer analogs termed α-galactosylsphingamides that contain a phenyl group connected to the phytosphingosine moiety via an amide linker. The rationale was that the phenyl groups would act as an anchor to increase the binding interaction with CD1d, while not affecting the interaction with the TCR of iNKT cells. Unexpectedly, although the TCR bound the sphingamides with high affinity, short acyl chain (C8-C12) αGSAs failed to activate iNKT cells in vitro and in vivo, while long acyl chain αGSAs conferred antigenicity. The obvious conundrum was that both short chain (inactive) and long chain (active) αGSAs showed no difference in the TCR binding kinetics, as determined by surface plasmon resonance studies using recombinant molecules in solution. Even though, this assay does not account for other interactions (e.g. co-receptor binding, formation of the immunological synapse) that would occur in vivo upon antigen recognition, previous studies on NKT cells observed a correlation between the 2D-TCR binding affinity and the cytokine production (5,7,31-33). By determining the crystal structures of various αGSAs and control compounds before and after TCR binding we identified a molecular switch that controls the antigenicity of αGSAs, yet does not affect the TCR binding kinetics. The molecular switch is formed between the amide oxygen of the αGSAs and Tyr73 of CD1d and controlled by the acyl chain length of the ligands. This molecular switch has an "ON" and "OFF" position before TCR binding, which correlates with the subsequent ability to activate NKT cells. Considering that there is no difference in the TCR binding kinetics between inactive and active αGSAs, we speculate that a compensatory mechanism is masking the biophysical properties leading to the observed biological differences. The active sphingamide αGSA[26P5*p*] with an in-chain phenyl group is an outlier, since it lacks the pre-formed H bond with Tyr73 but also has reduced TCR binding affinity. Previously we had reported that the TCR association rate toward CD1d-glycolipid complexes is affected by the positioning of the galactose moiety (29). Since α-GalCer is already presented in the ideal orientation, a fast TCR association rate is observed, while ligands that need to undergo a re-orientation of the sugar upon TCR binding have a slower association rate(29). TCR dissociation is affected by whether the F' roof is open or closed before TCR binding (29). For αGSAs, TCR binding positioned the amide group in a way that the amide oxygen formed the novel H bond interaction with Tyr73 of CD1d. We believe that this interaction stabilized TCR binding (and reduced dissociation), since CD1d itself contributed binding energy to keep the amide group in place. As such, we did not see reduced TCR dissociation. A similar scenario was reported for α-glycosyl diacylglycerolipids from *S. pneumoniae* in comparison to α-galactosyl diacylglycerolipids from *B. burgdorferi.* Here, the TCR dissociated much slower from the glucose containing ligand compared to the galactose containing ligand (34). This was likely due to a novel contact formed between the glucose-specific axial 4"-OH and Thr156 of CD1d, which cannot be formed with the galactose version (34). Overall, the binding affinity between both galactose and glucose antigens was similar.

Interestingly, a similar phenomenon was recently described for peptide-(p)MHC restricted TCRs. Here, TCRs were also found to bind with high affinity to pMHC complexes, yet this binding event did not lead to T cell activation (35). Using single-molecule force measurements, the authors demonstrated the emergence of catch bonds in the activating pMHC-TCR interface, while non-agonist peptides formed slip bonds with the same TCR under force, which accounted for the differences in T cell activation (35).

Recently p-MeOBz amide-containing α-GalCer analogs have been reported that contain aromatic groups within the acyl chain but also carry an amide linker, as well as an additional oxygen following the aromatic group. The polar amide was designed to interact with a region in the A´ pocket of CD1d that for

a slightly polar side pocket (Ser28 and Gln14) (36). Surprisingly, the incorporation of polar groups within the acyl chain results in a Th2 polarized NKT cell response characterized by a reduced production of IFN-g and increased levels of IL-4. Therefore, the incorporation of polar moieties in an otherwise apolar glycolipid antigen is a novel strategy for modulation NKT cell responses but the outcome of the associated immune response is difficult to predict at this point.

The sphingamides are also of interest for the development of NKT cell antagonists, if their binding affinity towards CD1d can be increased, without leading to antigenicity. Such a sphingamide would contain the short acyl chain (for inactivity) but introduce a third anchor, such as we have identified in the glycolipid NU-α-GalCer (16). Development of NKT cell antagonists using short chain sphingamides as a scaffold are currently ongoing.

EXPERIMENTAL PROCEDURES

Protein expression and purification- Mouse CD1d/b2M was expressed in *Spodoptera frugiperda* (*Sf*9) insect cells using the baculovirus expression system and purified as previously reported (5). The Vα14Vβ8.2 TCR from the iNKT cell hybridoma 2C12 was generated by expressing the separate TCR α and β chains in *E. coli* and refolding from inclusion bodies as reported (5).

Lipid synthesis- α-Galactosylceramides containing either a C8 or C26 fatty acyl chain and sphingosine chains of varying length with terminal phenyl moieties were synthesized as reported (37). α-Galactosylsphingamides were synthesized as previously reported (28). Structural representations of all lipids are found in Figure 1.

Surface Plasmon Resonance studies- For kinetic experiments, enzymatically biotinylated CD1d (C-terminal birA tag) was used for lipid loading (see next chapter). Individual CD1d-glycolipid complexes were immobilized on a CAP sensor chip (GE Healthcare, Chicago, IL) at levels between 100-400 response units using a Biacore T200. Increasing concentrations of TCR (15 nM to 1 μM) in HBS-EP buffer (10 mM HEPES, 150 mM NaCl, 3 mM EDTA and 0.05% surfactant Tween 20) were passed over the sensor chip at a flowrate of 30 μl/min, without regenerating the sensor chip surface in between cycles. Association was observed for 4 min, while dissociation was continued for up to 15 min. All binding curves were corrected for background and bulk refractive index contribution by subtracting the response of the reference flow cells from the active surface. Kinetic data were analyzed using the Biacore T200 Evaluation software 2.0 (GE Healthcare, Chicago, IL) using a 1:1 Langmuir interaction kinetic model in order to calculate the association rate (k_a) and the dissociation rate (k_d) and the equilibrium dissociation constant ($K_D = k_d/k_a$) by non-linear fitting. Kinetic experiments were performed at least twice with 2 different TCR preparations.

Antigen presentation assay- The cell-free antigen-presentation assay has been performed as reported (38). 96-well plates were coated with 1 μg of CD1d and incubated overnight at RT with three different concentrations of glycolipids as triplicates. Buffer was removed and hybridoma cells ($5x10^4$) in culture media were added to each well and co-incubated with CD1d-glicolipid complexes overnight at 37˚C in a CO_2 incubator. The cell-based antigen-presentation assay also has been described (39). Briefly, antigen-presenting cells ($1x10^5$ per well) were pulsed with indicated amounts of glycolipid and were incubated overnight. The cells were then combined with $5x10^4$ cells of the Vα14Vβ8.2 NKT cell hybridoma DN3A4-1.2 (1.2) for 24 h. The 1.2 type I NKT hybridoma cell line has been described previously (40). TCR stimulation and T cell activation was measured using a sandwich ELISA for IL-2 cytokines in the supernatant of hybridoma cultures.

Lipid loading, complex formation and crystallization- Mouse CD1d was incubated with a 6-10 fold molar excess of glycolipids (dissolved in DMSO at 10 mg/ml) in 50 mM Hepes pH 7.5, 150 mM NaCl and incubated over night at room temperature (RT) under slight agitation. For structural analysis of CD1d-glycolipid complexes, the CD1d/lipid mixture was spun down (14,000 g at 4˚C for 10 min), concentrated using 30 kDa molecular filtration devices and purified further by size exclusion chromatography using a Superdex S-200 GL10/300 column. For structural analysis of CD1d-glycolipid-TCR complexes, the CD1d-lipid mixtures were incubated for 2h at RT with purified TCR at 2-fold molar excess of CD1d, concentrated to ~250 μl and subjected to SEC to separate ternary complexes from unbound CD1d and TCR using a Superdex S-200 GL10/300. Fractions containing CD1d-glycolipid or CD1d-glycolipid-TCR complexes were pooled, concentrated to ~5 mg/ml in 10 mM HEPES pH 7.5, 30 mM NaCl and subjected to crystallization trials using the sitting drop vapor diffusion method. Typically, 1 μl of protein solution was mixed with 1 μl precipitant using selected conditions of the PEG/ION screen that previously

yielded crystals of related CD1d-glycolipid or CD1d-glycolipid-TCR complexes. Plates were incubated at 22.3˚C for several days (ternary complexes) or 1-2 weeks (CD1d-glycolipid) before harvesting individual crystals for diffraction analysis. Crystallization conditions for each individual complex are listed in Table S1.

Data collection and structure determination- Single crystals were cryo-protected by immersion in crystallization solution containing 20-25% glycerol and flash cooled in liquid nitrogen. Diffraction data were collected remotely at beam line 7-1, 14-1 and 9-2 at the Stanford Synchrotron Radiation Light source (SSRL, Menlo Park, CA). Diffraction data for the individual crystals were processed and scaled using HKL2000. All structures were determined by molecular replacement method using the protein coordinates from the mCD1d-iGb3 structure (PDB ID 2Q7Y) and in case of ternary complexes also the TCR coordinates (PDB ID 3QUZ) using PHASER (41) as part of the CCP4 suite (42). The models were built in COOT (43) and iteratively refined using REFMAC5 (44).Refinement progress was monitored by a continuous drop in R_{free} values and improvement in electron density. Data collection and refinement statistics are presented in Table S1. The quality of the models was examined using Molprobity (45). Crystal structure illustrations were prepared using MacPyMOL (Schroedinger, New York City, NY).

Accession numbers. The coordinates and structure factors of the various complexes have been deposited in the Protein Data Bank (www.rcsb.org), under the accession codes listed in Table S1.

Conflict of interest: The authors declare that the research was conducted in the absence of any commercial or financial relationships that could be construed as a potential conflict of interest.

Author contributions: JW, JG, JJ, SGR, GY, AB, and DMZ performed experiments and analyzed the data. SVC conceived the overall project with DMZ and edited the paper. DMZ conceived the experiments, supervised the overall project and wrote the manuscript.

Footnotes

Use of the Stanford Synchrotron Radiation Lightsource, SLAC National Accelerator Laboratory, is supported by the U.S. Department of Energy, Office of Science, Office of Basic Energy Sciences under Contract No. DE-AC02-76SF00515. The SSRL Structural Molecular Biology Program is supported by the DOE Office of Biological and Environmental Research, and by the National Institutes of Health, National Institute of General Medical Sciences (including P41GM103393). The contents of this publication are solely the responsibility of the authors and do not necessarily represent the official views of NIGMS or NIH. This work was supported in part by the National Institute of Health grant AI137230 to DMZ.

REFERENCES

1. Bendelac, A., Savage, P. B., and Teyton, L. (2007) The Biology of NKT Cells. *Annu Rev Immunol* **25**, 297-336
2. Yu, E. D., Girardi, E., Wang, J., and Zajonc, D. M. (2011) Cutting Edge: Structural Basis for the Recognition of {beta}-Linked Glycolipid Antigens by Invariant NKT Cells. *J Immunol* **187**, 2079-2083
3. Mallevaey, T., Clarke, A. J., Scott-Browne, J. P., Young, M. H., Roisman, L. C., Pellicci, D. G., Patel, O., Vivian, J. P., Matsuda, J. L., McCluskey, J., Godfrey, D. I., Marrack, P., Rossjohn, J., and Gapin, L. (2011) A molecular basis for NKT cell recognition of CD1d-self-antigen. *Immunity* **34**, 315-326
4. Godfrey, D. I., Pellicci, D. G., and Rossjohn, J. (2011) Beta-testing NKT cell self-reactivity. *Nat Immunol* **12**, 1135-1137
5. Wang, J., Li, Y., Kinjo, Y., Mac, T. T., Gibson, D., Painter, G. F., Kronenberg, M., and Zajonc, D. M. (2010) Lipid binding orientation within CD1d affects recognition of Borrelia burgorferi antigens by NKT cells. *Proc Natl Acad Sci U S A* **107**, 1535-1540
6. Schiefner, A., Fujio, M., Wu, D., Wong, C. H., and Wilson, I. A. (2009) Structural evaluation of potent NKT cell agonists: implications for design of novel stimulatory ligands. *J Mol Biol* **394**, 71-82
7. Silk, J. D., Salio, M., Reddy, B. G., Shepherd, D., Gileadi, U., Brown, J., Masri, S. H., Polzella, P., Ritter, G., Besra, G. S., Jones, E. Y., Schmidt, R. R., and Cerundolo, V. (2008) Cutting edge: nonglycosidic CD1d lipid ligands activate human and murine invariant NKT cells. *J Immunol* **180**, 6452-6456
8. Wu, D., Xing, G. W., Poles, M. A., Horowitz, A., Kinjo, Y., Sullivan, B., Bodmer-Narkevitch, V., Plettenburg, O., Kronenberg, M., Tsuji, M., Ho, D. D., and Wong, C. H. (2005) Bacterial glycolipids and analogs as antigens for CD1d-restricted NKT cells. *Proc Natl Acad Sci U S A* **102**, 1351-1356
9. Kinjo, Y., and Kronenberg, M. (2005) V alpha14 i NKT cells are innate lymphocytes that participate in the immune response to diverse microbes. *J Clin Immunol* **25**, 522-533
10. Skold, M., and Behar, S. M. (2003) Role of CD1d-restricted NKT cells in microbial immunity. *Infect Immun* **71**, 5447-5455
11. Sidobre, S., Naidenko, O. V., Sim, B. C., Gascoigne, N. R., Garcia, K. C., and Kronenberg, M. (2002) The Vα14 NKT cell TCR exhibits high-affinity binding to a glycolipid/CD1d complex. *J Immunol* **169**, 1340-1348
12. Kawano, T., Cui, J., Koezuka, Y., Toura, I., Kaneko, Y., Motoki, K., Ueno, H., Nakagawa, R., Sato, H., Kondo, E., Koseki, H., and Taniguchi, M. (1997) CD1d-restricted and TCR-mediated activation of Vα14 NKT cells by glycosylceramides. *Science* **278**, 1626-1629
13. Kain, L., Webb, B., Anderson, B. L., Deng, S., Holt, M., Costanzo, A., Zhao, M., Self, K., Teyton, A., Everett, C., Kronenberg, M., Zajonc, D. M., Bendelac, A., Savage, P. B., and Teyton, L. (2014) The identification of the endogenous ligands of natural killer T cells reveals the presence of mammalian alpha-linked glycosylceramides. *Immunity* **41**, 543-554
14. Carreno, L. J., Saavedra-Avila, N. A., and Porcelli, S. A. (2016) Synthetic glycolipid activators of natural killer T cells as immunotherapeutic agents. *Clin Transl Immunology* **5**, e69
15. Schmieg, J., Yang, G., Franck, R. W., and Tsuji, M. (2003) Superior protection against malaria and melanoma metastases by a C-glycoside analogue of the natural killer T cell ligand α-Galactosylceramide. *J Exp Med* **198**, 1631-1641
16. Aspeslagh, S., Li, Y., Yu, E. D., Pauwels, N., Trappeniers, M., Girardi, E., Decruy, T., Van Beneden, K., Venken, K., Drennan, M., Leybaert, L., Wang, J., Franck, R. W., Van Calenbergh, S., Zajonc, D. M., and Elewaut, D. (2011) Galactose-modified iNKT cell agonists stabilized by an induced fit of CD1d prevent tumour metastasis. *Embo J* **30**, 2294-2305
17. Aspeslagh, S., Nemcovic, M., Pauwels, N., Venken, K., Wang, J., Van Calenbergh, S., Zajonc, D. M., and Elewaut, D. (2013) Enhanced TCR footprint by a novel glycolipid increases NKT-dependent tumor protection. *J Immunol* **191**, 2916-2925
18. Wesley, J. D., Tessmer, M. S., Chaukos, D., and Brossay, L. (2008) NK cell-like behavior of Valpha14i NK T cells during MCMV infection. *PLoS Pathog* **4**, e1000106
19. Smyth, M. J., Crowe, N. Y., Pellicci, D. G., Kyparissoudis, K., Kelly, J. M., Takeda, K., Yagita, H., and Godfrey, D. I. (2002) Sequential production of interferon-gamma by NK1.1(+) T cells and natural killer cells is essential for the antimetastatic effect of alpha-galactosylceramide. *Blood* **99**, 1259-1266

20. Sullivan, B. A., Nagarajan, N. A., Wingender, G., Wang, J., Scott, I., Tsuji, M., Franck, R. W., Porcelli, S. A., Zajonc, D. M., and Kronenberg, M. (2010) Mechanisms for glycolipid antigen-driven cytokine polarization by Vα14i NKT cells. *J Immunol* **184**, 141-153
21. Im, J. S., Arora, P., Bricard, G., Molano, A., Venkataswamy, M. M., Baine, I., Jerud, E. S., Goldberg, M. F., Baena, A., Yu, K. O., Ndonye, R. M., Howell, A. R., Yuan, W., Cresswell, P., Chang, Y. T., Illarionov, P. A., Besra, G. S., and Porcelli, S. A. (2009) Kinetics and cellular site of glycolipid loading control the outcome of natural killer T cell activation. *Immunity* **30**, 888-898
22. Birkholz, A., Nemcovic, M., Yu, E. D., Girardi, E., Wang, J., Khurana, A., Pauwels, N., Farber, E., Chitale, S., Franck, R. W., Tsuji, M., Howell, A., Van Calenbergh, S., Kronenberg, M., and Zajonc, D. M. (2015) Lipid and Carbohydrate Modifications of alpha-Galactosylceramide Differently Influence Mouse and Human Type I Natural Killer T Cell Activation. *J Biol Chem* **290**, 17206-17217
23. Padte, N. N., Li, X., Tsuji, M., and Vasan, S. (2011) Clinical development of a novel CD1d-binding NKT cell ligand as a vaccine adjuvant. *Clinical immunology* **140**, 142-151
24. Li, X., Fujio, M., Imamura, M., Wu, D., Vasan, S., Wong, C. H., Ho, D. D., and Tsuji, M. (2010) Design of a potent CD1d-binding NKT cell ligand as a vaccine adjuvant. *Proceedings of the National Academy of Sciences of the United States of America* **107**, 13010-13015
25. Coelho-Dos-Reis, J. G., Li, X., and Tsuji, M. (2018) Development of a novel mechanism-based glycolipid adjuvant for vaccination. *F1000Res* **7**
26. Li, X., Huang, J., Kaneko, I., Zhang, M., Iwanaga, S., Yuda, M., and Tsuji, M. (2017) A potent adjuvant effect of a CD1d-binding NKT cell ligand in human immune system mice. *Expert Rev Vaccines* **16**, 73-80
27. Zajonc, D. M., Cantu, C., Mattner, J., Zhou, D., Savage, P. B., Bendelac, A., Wilson, I. A., and Teyton, L. (2005) Structure and function of a potent agonist for the semi-invariant natural killer T cell receptor. *Nat Immunol* **8**, 810-818
28. Guillaume, J., Wang, J., Janssens, J., Remesh, S. G., Risseeuw, M. D. P., Decruy, T., Froeyen, M., Elewaut, D., Zajonc, D. M., and Calenbergh, S. V. (2017) Galactosylsphingamides: new alpha-GalCer analogues to probe the F'-pocket of CD1d. *Sci Rep* **7**, 4276
29. Li, Y., Girardi, E., Wang, J., Yu, E. D., Painter, G. F., Kronenberg, M., and Zajonc, D. M. (2010) The Vα14 invariant natural killer T cell TCR forces microbial glycolipids and CD1d into a conserved binding mode. *J Exp Med* **207**, 2383-2393
30. Scott-Browne, J. P., Matsuda, J. L., Mallevaey, T., White, J., Borg, N. A., McCluskey, J., Rossjohn, J., Kappler, J., Marrack, P., and Gapin, L. (2007) Germline-encoded recognition of diverse glycolipids by natural killer T cells. *Nat Immunol* **8**, 1105-1113
31. Wun, K. S., Cameron, G., Patel, O., Pang, S. S., Pellicci, D. G., Sullivan, L. C., Keshipeddy, S., Young, M. H., Uldrich, A. P., Thakur, M. S., Richardson, S. K., Howell, A. R., Illarionov, P. A., Brooks, A. G., Besra, G. S., McCluskey, J., Gapin, L., Porcelli, S. A., Godfrey, D. I., and Rossjohn, J. (2011) A molecular basis for the exquisite CD1d-restricted antigen specificity and functional responses of natural killer T cells. *Immunity* **34**, 327-339
32. McCarthy, C., Shepherd, D., Fleire, S., Stronge, V. S., Koch, M., Illarionov, P. A., Bossi, G., Salio, M., Denkberg, G., Reddington, F., Tarlton, A., Reddy, B. G., Schmidt, R. R., Reiter, Y., Griffiths, G. M., van der Merwe, P. A., Besra, G. S., Jones, E. Y., Batista, F. D., and Cerundolo, V. (2007) The length of lipids bound to human CD1d molecules modulates the affinity of NKT cell TCR and the threshold of NKT cell activation. *J Exp Med* **204**, 1131-1144
33. Kinjo, Y., Tupin, E., Wu, D., Fujio, M., Garcia-Navarro, R., Benhnia, M. R., Zajonc, D. M., Ben-Menachem, G., Ainge, G. D., Painter, G. F., Khurana, A., Hoebe, K., Behar, S. M., Beutler, B., Wilson, I. A., Tsuji, M., Sellati, T. J., Wong, C. H., and Kronenberg, M. (2006) Natural killer T cells recognize diacylglycerol antigens from pathogenic bacteria. *Nat Immunol* **7**, 978-986
34. Girardi, E., Yu, E. D., Li, Y., Tarumoto, N., Pei, B., Wang, J., Illarionov, P., Kinjo, Y., Kronenberg, M., and Zajonc, D. M. (2011) Unique interplay between sugar and lipid in determining the antigenic potency of bacterial antigens for NKT cells. *PLoS biology* **9**, e1001189
35. Sibener, L. V., Fernandes, R. A., Kolawole, E. M., Carbone, C. B., Liu, F., McAffee, D., Birnbaum, M. E., Yang, X., Su, L. F., Yu, W., Dong, S., Gee, M. H., Jude, K. M., Davis, M. M., Groves, J. T., Goddard, W. A., 3rd, Heath, J. R., Evavold, B. D., Vale, R. D., and Garcia, K. C. (2018) Isolation of a Structural Mechanism for Uncoupling T Cell Receptor Signaling from Peptide-MHC Binding. *Cell* **174**, 672-687 e627

36. Kishi, J., Inuki, S., Hirata, N., Kashiwabara, E., Yoshidome, D., Ichihara, O., and Fujimoto, Y. (2019) Structure-activity relationship studies of Bz amide-containing alpha-GalCer derivatives as natural killer T cell modulators. *Bioorg Med Chem Lett* **29**, 970-973
37. Niu, Y., Cao, X., and Ye, X.-S. (2008) Improved Synthesis of Phytosphingosine and Dihydrosphingosine from 3,4,6-Tri-O-benzyl-D-galactal. *Helvetica Chimica Acta* **91**, 746-752
38. Naidenko, O. V., Maher, J. K., Ernst, W. A., Sakai, T., Modlin, R. L., and Kronenberg, M. (1999) Binding and antigen presentation of ceramide-containing glycolipids by soluble mouse and human CD1d molecules. *J Exp Med* **190**, 1069-1080.
39. Lawton, A. P., Prigozy, T. I., Brossay, L., Pei, B., Khurana, A., Martin, D., Zhu, T., Spate, K., Ozga, M., Honing, S., Bakke, O., and Kronenberg, M. (2005) The mouse CD1d cytoplasmic tail mediates CD1d trafficking and antigen presentation by adaptor protein 3-dependent and -independent mechanisms. *J Immunol* **174**, 3179-3186
40. Brossay, L., Tangri, S., Bix, M., Cardell, S., Locksley, R., and Kronenberg, M. (1998) Mouse CD1-autoreactive T cells have diverse patterns of reactivity to CD1+ targets. *Journal of immunology* **160**, 3681-3688
41. McCoy, A. J., Grosse-Kunstleve, R. W., Storoni, L. C., and Read, R. J. (2005) Likelihood-enhanced fast translation functions. *Acta Crystallogr.* **D61**, 458-464
42. CCP4. (1994) Collaborative Computational Project, Number 4. The CCP4 Suite: Programs for Protein Crystallography. *Acta Crystallogr.* **D50**, 760-763
43. Emsley, P., and Cowtan, K. (2004) Coot: model-building tools for molecular graphics. *Acta Crystallogr D Biol Crystallogr* **60**, 2126-2132
44. Murshudov, G. N., Vagin, A. A., and Dodson, E. J. (1997) Refinement of macromolecular structures by the maximum likelihood method. *Acta Crystallogr.* **D53**, 240-255
45. Lovell, S. C., Davis, I. W., Arendall, W. B., 3rd, de Bakker, P. I., Word, J. M., Prisant, M. G., Richardson, J. S., and Richardson, D. C. (2003) Structure validation by Cα geometry: ϕ,ψ and Cβ deviation. *Proteins* **50**, 437-450

FIGURE LEGENDS

Figure 1. Overview of glycolipids. Sphingamides (αGSAs) (middle panel) were structurally derived from the short chain α-GalCer analog (αGC[8,18]) with increasing alkyl chain length between the terminal phenyl anchor and the amide group. The αGSA was then selected and variants synthesized with acyl chain length from C12 to C26 (left panel). Control α-GalCer analogs with terminal phenyl anchors lacking the amide group were also prepared (right column). Bottom row, αGSAs that have a short or long acyl chain and a central phenyl anchor.

Figure 2. TCR binding kinetics. SPR sensorgrams are shown as red curves with fitted data (1:1 Langmuir interaction) shown as black curves. TCR concentrations are indicated and inset show the kinetic data including TCR association rate (k_a), TCR dissociation rate (k_d) and equilibrium binding constant (K_D). Each binding experiment was performed at least twice with 2 different TCR preparations. One representative sensorgram is shown.

Figure 3. NKT cell activation by sphingamides. Short chain αGSAs were assessed for their ability to induce IL-2 production by the murine NKT cell hybridoma 1.2 when added to recombinant mCD1d (A), or when added to A20 cells that were transfected with either tail-deleted CD1d (B), or wildtype CD1d (C). IL-2 was measured in the supernatant using ELISA. GalGalCer was used as a control for CD1d trafficking through the lysosome. D, same as A but including long chain αGSAs and a higher antigen concentration dose. Experiments were performed at least 3 times with one representative experiments shown.

Figure 4. Glycolipid binding orientation in mCD1d. Overview of the CD1d-glycolipid structure (top left). Side view of the CD1d binding groove with the α2-helix removed for better view. CD1d in grey cartoon, glycolipids as yellow sticks, and colored by atom type. Several CD1d residues that are responsible for lipid binding are depicted. Electron density (2FoFc at 1σ) is shown only for the glycolipids. Spacer lipid shown in green.

Figure 5. H bond network between CD1d and glycolipids. Detailed view into the binding groove of CD1d (grey cartoon), with glycolipids as yellow sticks and colored by atom type. CD1d residues that form H bond interactions with the antigen are depicted. H bonds shown as dashed blue lines (3.5 Å distance cut-off). Spacer lipid shown in green. Note that the novel H bond is only formed between the hydroxyl of Try73 of CD1d and the amide oxygen of the agonist αGSA[26,6P].

Figure 6. Overview of ternary complex structures with electron density for the glycolipids. Similar view and coloring as Figure 4 but with TCR α-chain shown as cyan cartoon and TCR β-chain shown as orange loops (not contacting the antigen). CDR1α and 3α sit above the glycolipid.

Figure 7. H bond interactions between TCR and glycolipid. Same color scheme as in Figure 5. TCR depicted as in Figure 6. Note that the novel H bond is formed between the hydroxyl of Try73 of CD1d with the amide oxygen in all sphingamide structures.

Figure 8. Molecular switch Tyr73 of CD1d modulates αGSA activity. Sphingamide binding comparison before (A) and after (B) TCR binding. αGSA (in different colors) are superimposed within the CD1d binding groove. αGSA[8,6P] in yellow and αGSA[26,6P] in cyan. αGSA[20,6P] in orange. Before TCR binding the sphingosine moiety of αGSA[26,6P] sits slightly deeper in the CD1d F′ pocket and forms the novel H bond with Tyr73. All αGSAs superimpose very well after TCR binding, with the only difference being the different acyl chains (B). Antigen-presentation assay by recombinant wildtype mCD1d or the mutants Y73F or Y73H similar to Figure 3. Increasing the acyl chain length from C8 to C26 increases the antigenicity of αGSAs. D. Crystal structure of the hyperactive mCD1d mutant Y73H bound to αGSA[8,6P] show the molecular switch in the “ON” position, correlating with the observed activity in panel C (right).

FIGURES

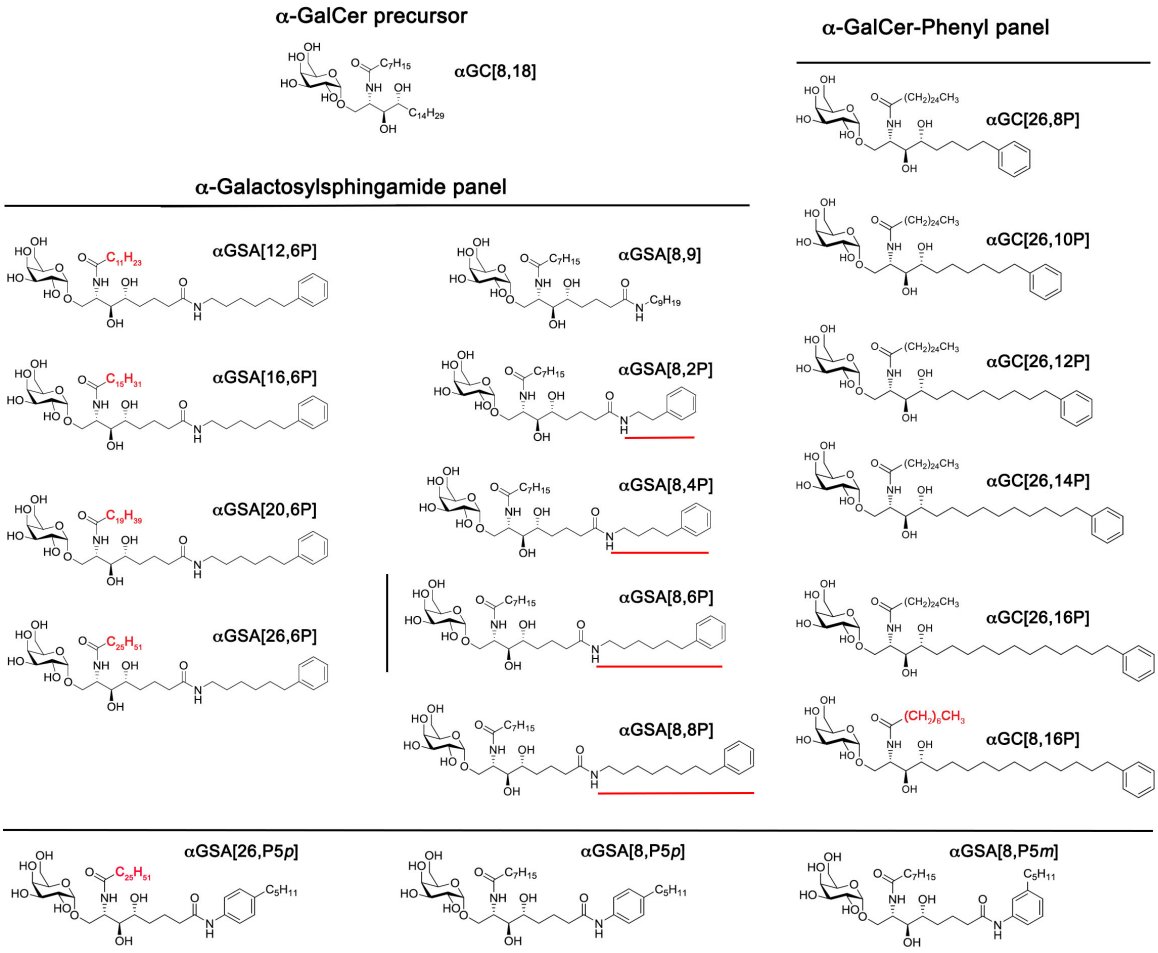

Figure 1.

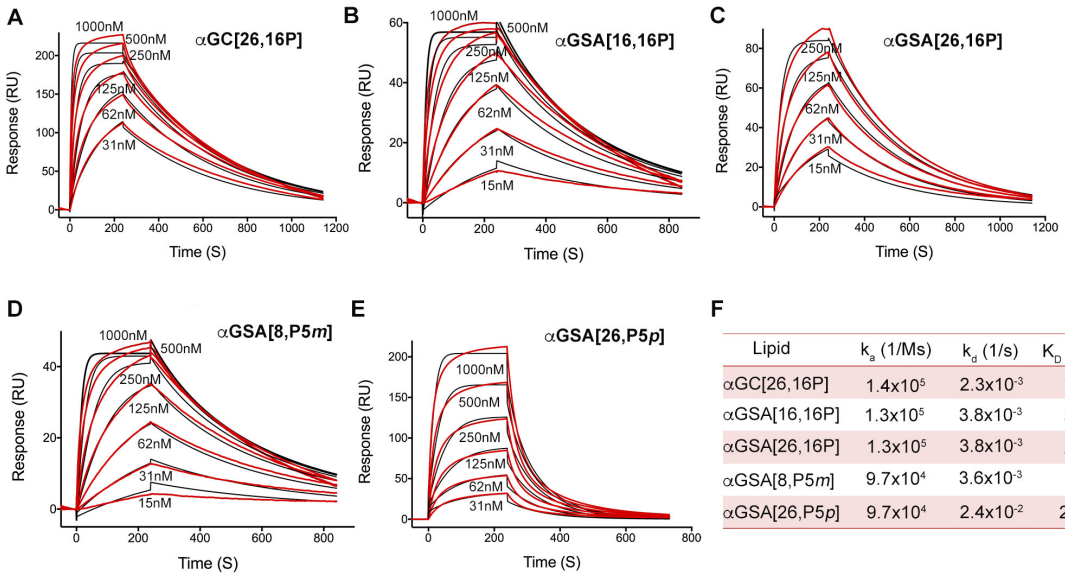

F

Lipid	k_a (1/Ms)	k_d (1/s)	K_D (nM)
αGC[26,16P]	$1.4x10^5$	$2.3x10^{-3}$	16
αGSA[16,16P]	$1.3x10^5$	$3.8x10^{-3}$	29
αGSA[26,16P]	$1.3x10^5$	$3.8x10^{-3}$	23
αGSA[8,P5*m*]	$9.7x10^4$	$3.6x10^{-3}$	37
αGSA[26,P5*p*]	$9.7x10^4$	$2.4x10^{-2}$	252

Figure 2.

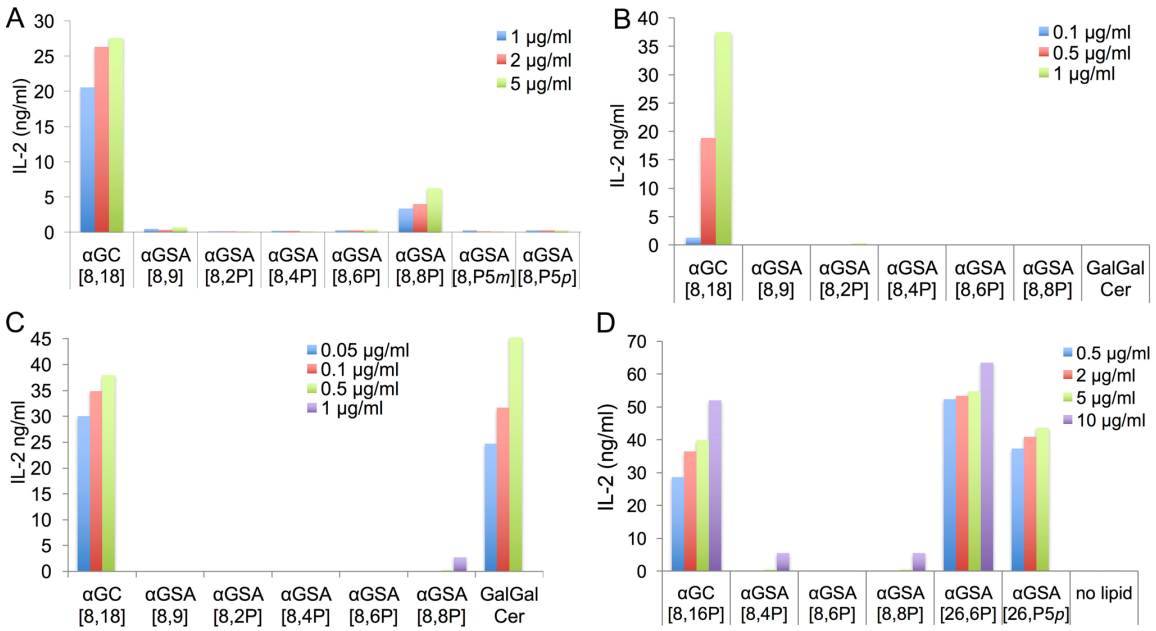
A
IL-2 (ng/ml)
1 µg/ml
2 µg/ml
5 µg/ml
αGC [8,18]
αGSA [8,9]
αGSA [8,2P]
αGSA [8,4P]
αGSA [8,6P]
αGSA [8,8P]
αGSA [8,P5m]
αGSA [8,P5p]
B
IL-2 ng/ml
0.1 µg/ml
0.5 µg/ml
1 µg/ml
αGC [8,18]
αGSA [8,9]
αGSA [8,2P]
αGSA [8,4P]
αGSA [8,6P]
αGSA [8,8P]
GalGal Cer
C
IL-2 ng/ml
0.05 µg/ml
0.1 µg/ml
0.5 µg/ml
1 µg/ml
αGC [8,18]
αGSA [8,9]
αGSA [8,2P]
αGSA [8,4P]
αGSA [8,6P]
αGSA [8,8P]
GalGal Cer
D
IL-2 (ng/ml)
0.5 µg/ml
2 µg/ml
5 µg/ml
10 µg/ml
αGC [8,16P]
αGSA [8,4P]
αGSA [8,6P]
αGSA [8,8P]
αGSA [26,6P]
αGSA [26,P5p]
no lipid

Figure 3.

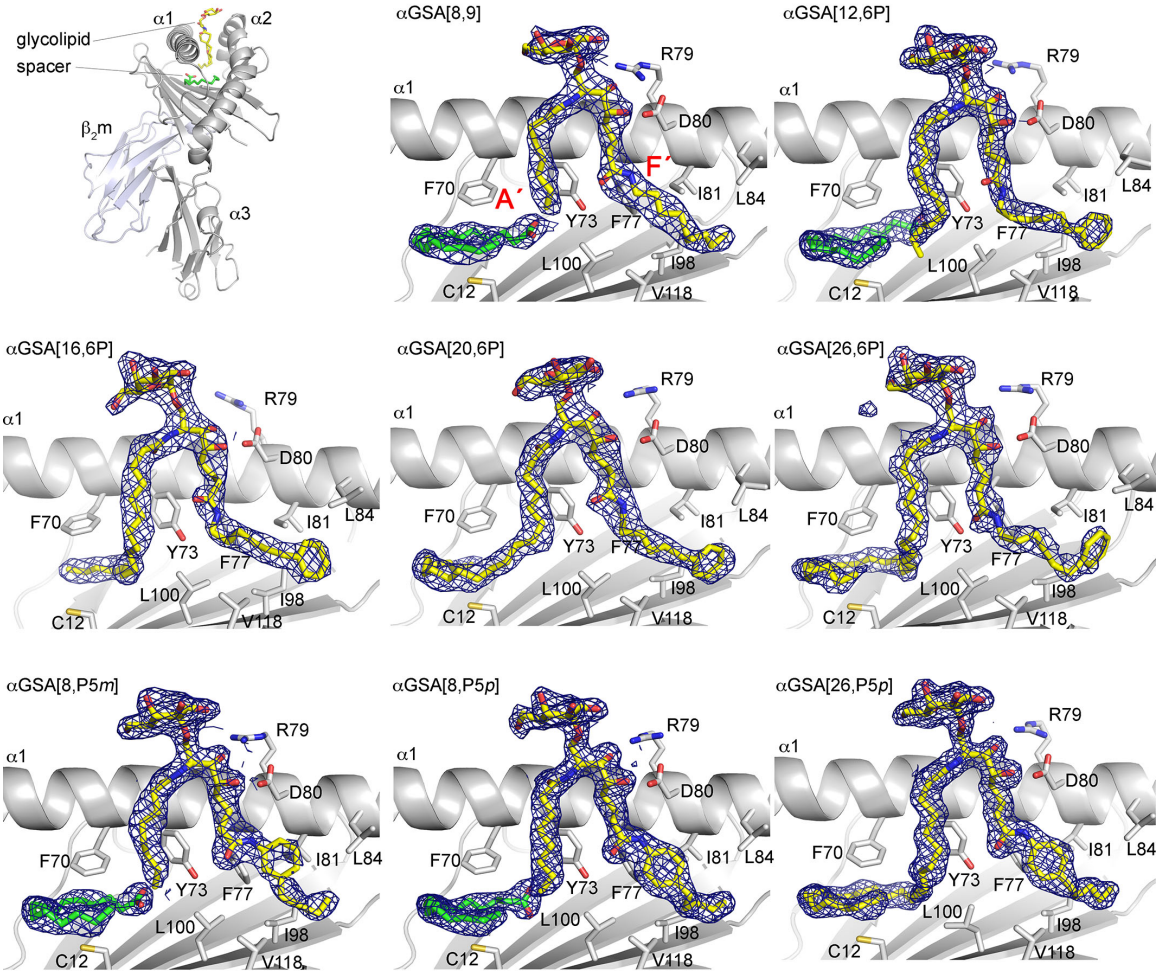
α1
α2
glycolipid
spacer
β2m
α3
αGSA[8,9]
αGSA[12,6P]
αGSA[16,6P]
αGSA[20,6P]
αGSA[26,6P]
αGSA[8,P5m]
αGSA[8,P5p]
αGSA[26,P5p]
R79
D80
F70
A´
F´
I81
L84
Y73
F77
L100
I98
C12
V118

Figure 4.

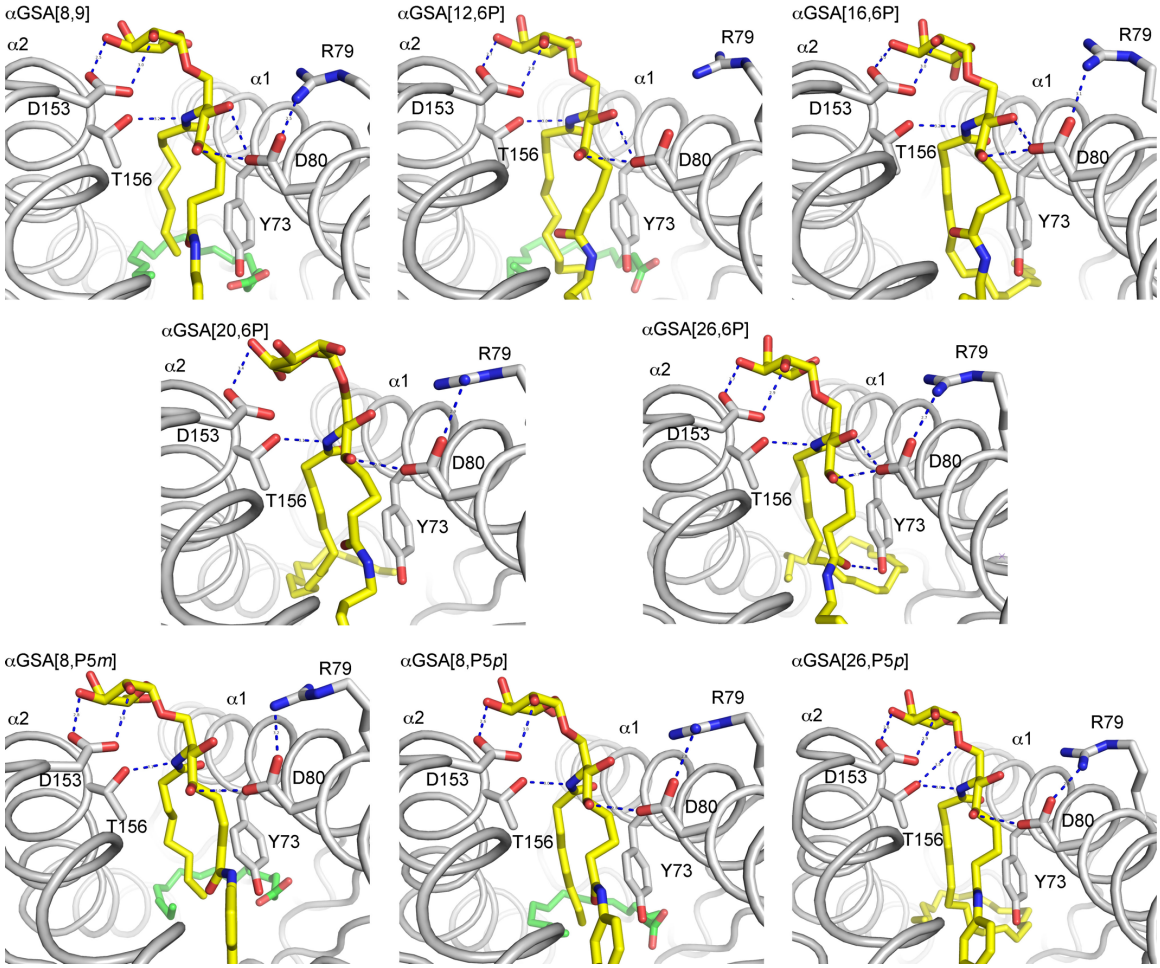
αGSA[8,9]
α2
α1
R79
D153
T156
D80
Y73
αGSA[12,6P]
α2
α1
R79
D153
T156
D80
Y73
αGSA[16,6P]
α2
α1
R79
D153
T156
D80
Y73
αGSA[20,6P]
α2
α1
R79
D153
T156
D80
Y73
αGSA[26,6P]
α2
α1
R79
D153
T156
D80
Y73
αGSA[8,P5m]
α2
α1
R79
D153
T156
D80
Y73
αGSA[8,P5p]
α2
α1
R79
D153
T156
D80
Y73
αGSA[26,P5p]
α2
α1
R79
D153
T156
D80
Y73

Figure 5.

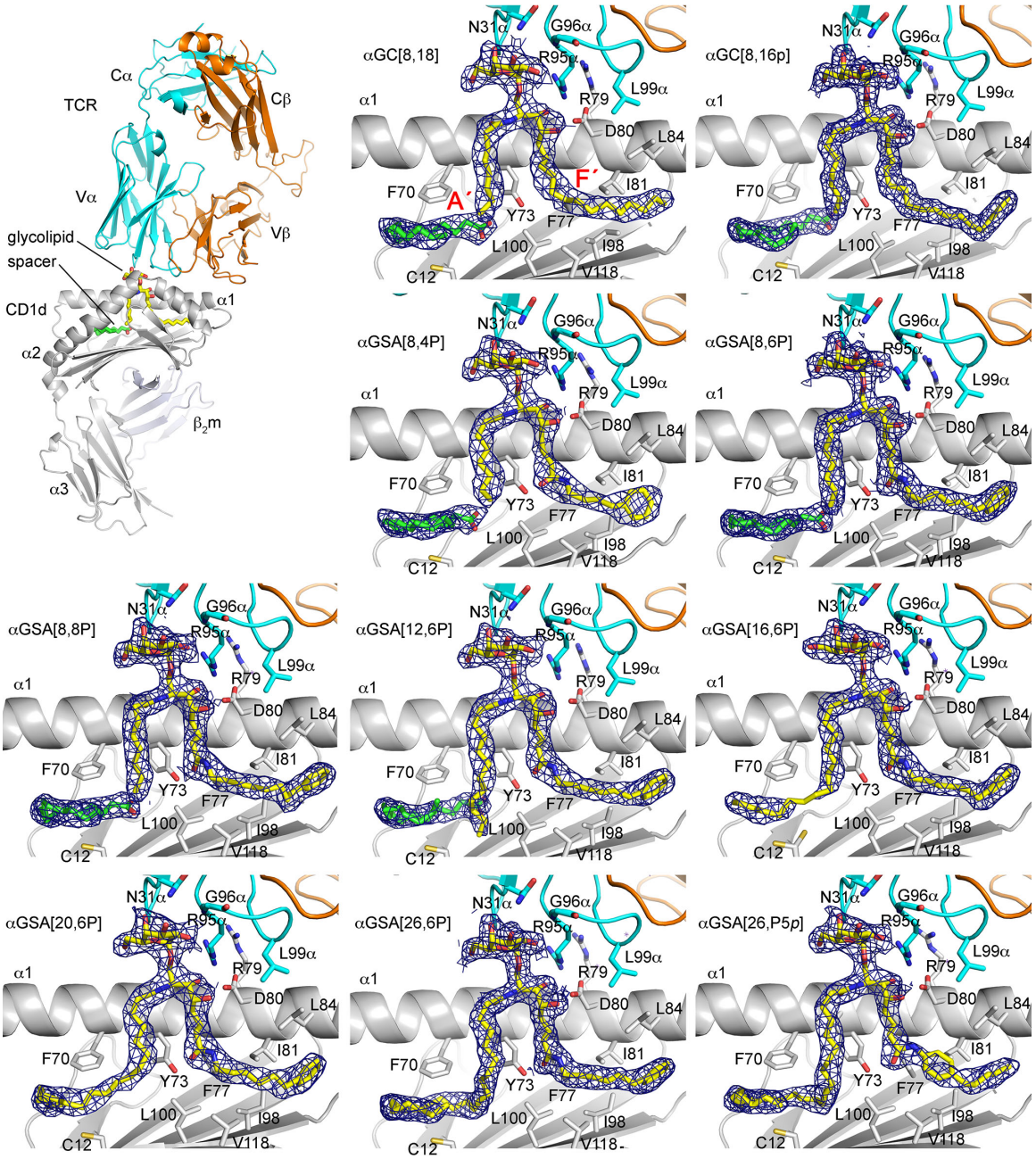
TCR
Cα
Cβ
Vα
Vβ
glycolipid
spacer
CD1d
α1
α2
α3
β2m
αGC[8,18]
αGC[8,16p]
αGSA[8,4P]
αGSA[8,6P]
αGSA[8,8P]
αGSA[12,6P]
αGSA[16,6P]
αGSA[20,6P]
αGSA[26,6P]
αGSA[26,P5p]
N31α
G96α
R95α
L99α
R79
D80
L84
I81
F70
Y73
F77
L100
I98
V118
C12
A′
F′

Figure 6.

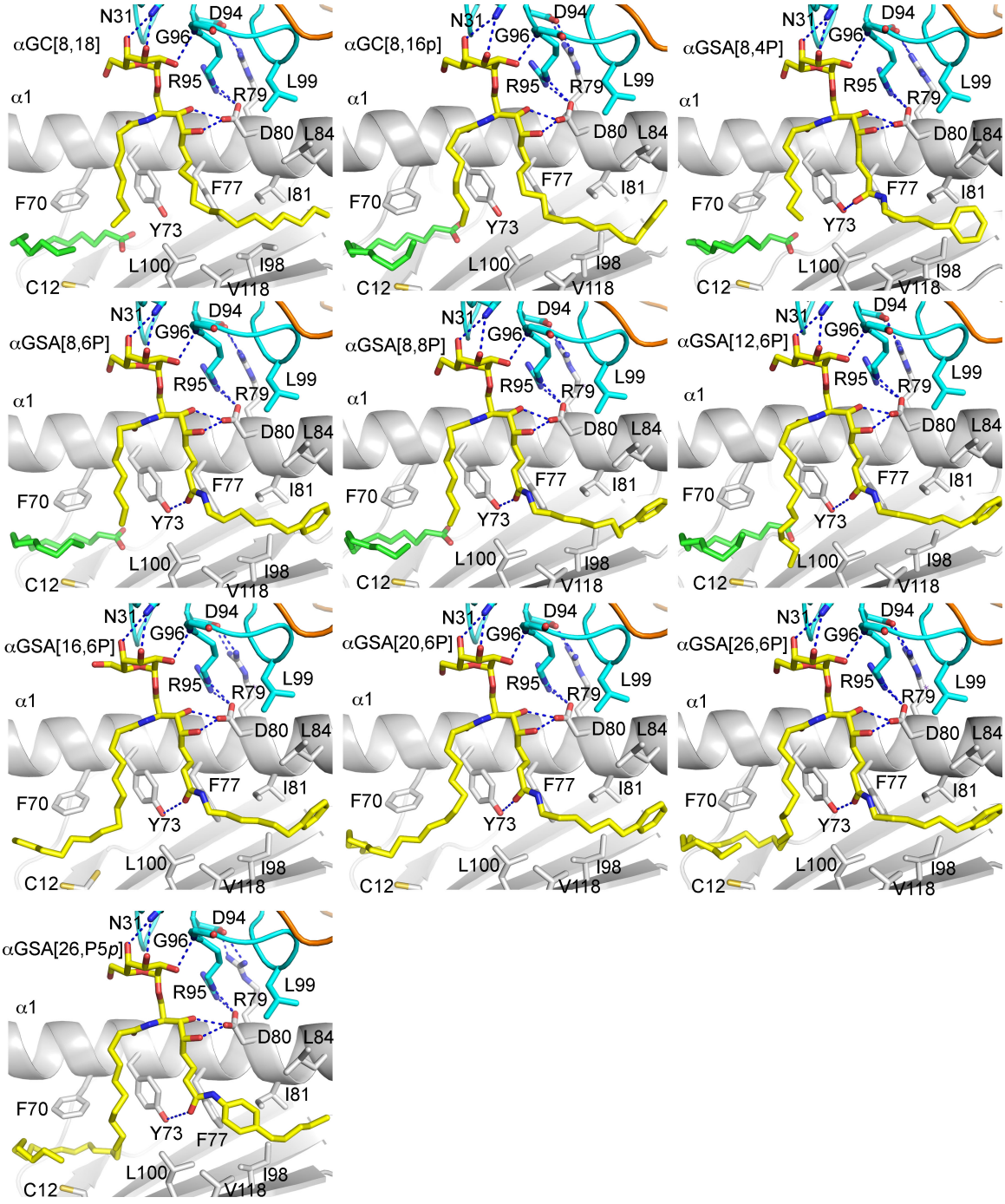
αGC[8,18]
αGC[8,16p]
αGSA[8,4P]
αGSA[8,6P]
αGSA[8,8P]
αGSA[12,6P]
αGSA[16,6P]
αGSA[20,6P]
αGSA[26,6P]
αGSA[26,P5p]
α1
N31
D94
G96
R95
R79
L99
D80
L84
F70
F77
I81
Y73
L100
I98
V118
C12

Figure 7.

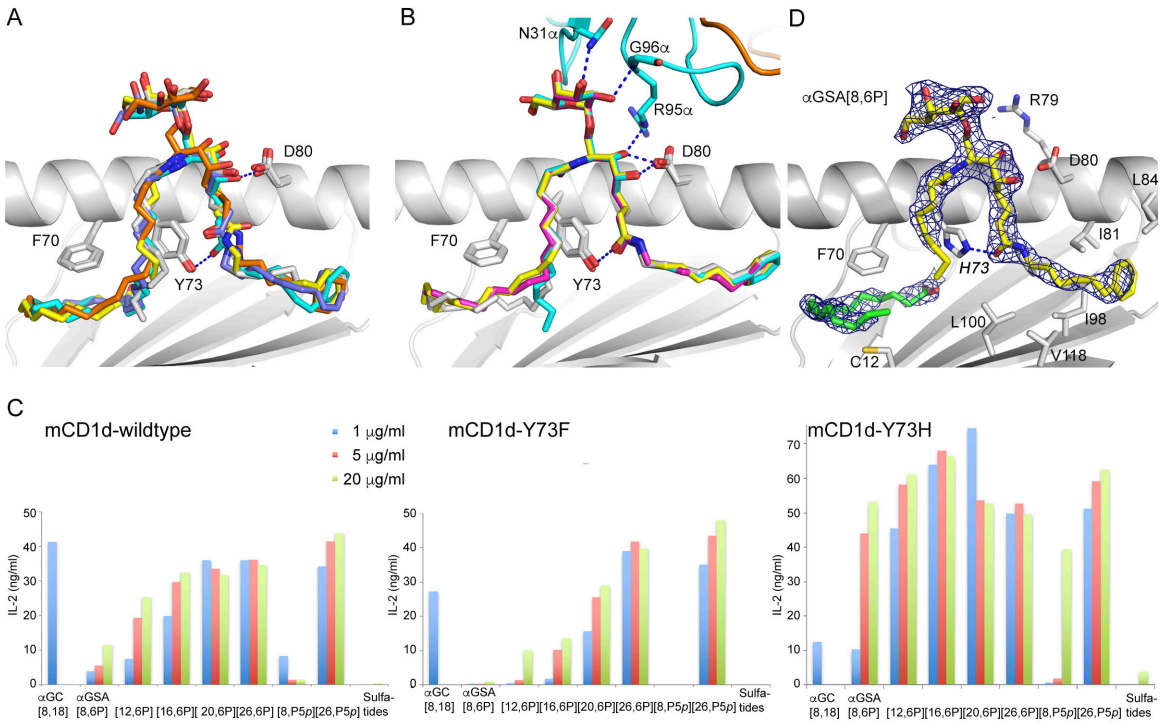
A
D80
F70
Y73
B
N31α
G96α
R95α
D80
F70
Y73
D
αGSA[8,6P]
R79
D80
L84
I81
F70
H73
L100
I98
C12
V118
C
mCD1d-wildtype
1 μg/ml
5 μg/ml
20 μg/ml
mCD1d-Y73F
mCD1d-Y73H
IL-2 (ng/ml)
αGC [8,18]
αGSA [8,6P]
[12,6P]
[16,6P]
[20,6P]
[26,6P]
[8,P5p]
[26,P5p]
Sulfa-tides

Figure 8.